Journal of ELECTRICAL ENGINEERING, VOL 73(2022), NO4, 226–236

sciendo

PAPERS

High-performance tri-band graphene plasmonic microstrip patch antenna using superstrate double-face metamaterial for THz communications

Sherif A. Khaleel[1,2], Ehab K. I. Hamad[2], Mohamed B. Saleh[1]

Recently, graphene-patch antennas have been widely used in communication technology, especially in THz applications due to the extraordinary properties of graphene material. Herein, a graphene-based rectangular microstrip patch antenna is designed on an FR4 substrate material ($\varepsilon_r = 4.3$). A single and double-faced superstrate MTM is placed upon the radiating patch for different purposes, such as enhancing the overall antenna performance, protecting the patch from environmental jeopardies, and generating a multiband resonance frequency. A single face superstrate triangle SRR unit was used to produce a dual-band frequency at 3.5 and 4.331 THz. The S_{11} of the dual-band structure is achieved to be -26.78 dB and -46.25 dB with a bandwidth of 400 GHz and 460 GHz, respectively. The double face superstrate MTM unit cell of the triangle SRR printed on the opposite face gives another resonant frequency, so, triple frequency bands of 2.32, 3.35, and 4.38 THz with a wide impedance bandwidth of 230, 520, and 610 GHz, were generated, respectively. The double-face superstrate MTM not only enhances the antenna performance but also generates another resonant frequency that could be used in the next 6G communications. The proposed antenna is designed and optimized using two commercial 3D full-wave software, CST Microwave Studio and Ansoft HFSS, to validate the results.

K e y w o r d s: double-face MTM, graphene, microstrip antenna, superstrate metamaterial, THz, triangle split ring resonator

1 Introduction

The fifth generation of communication has been completed and should be commercially launched in 2024 [1]. Therefore, the 6G communication systems developments should be taken into consideration for the future demand of 2030 [2]. This new revolution in communication technology needs a huge amount of data transmission and speed up to 10-100 Gb/s to meet the ever-increasing demand for speed [3]. Consequentially a special frequency band ranging from 0.1 to 10 THz is now considered crucial in solving the ever-increasing data rate demand. This band is the least studied frequency band. It supports extremely higher data rates, wider bandwidths, very high resolution, and size miniaturization of devices in the hundreds of gigahertz range [4]. Several types of antennas for terahertz band applications have been developed such as leaky wave antenna, bow-tie antenna, Yagi-Uda antenna, MEMS antenna, and planar microstrip patch antenna, [5]. The planar microstrip patch antenna has been used in different applications over the last decades due to its simple structure, low cost of production and can be easily integrated with other MMICs due to its possibility to be miniaturized to micrometer range. The metallic planar patch antenna suffers from a series of drawbacks such as low antenna efficiency, narrow bandwidth, low gain, and low-power handling capability [6]. This is due to low electron mobility in the metallic structure at the THz frequency band. To overcome this limitation, a graphene-based microstrip patch antenna is investigated in the terahertz frequency band. Graphene is an efficient material for THz applications due to its two-dimensional nature and unique electrical, mechanical, and optical properties [7]. The most important property of graphene is the ability to support the propagation of the surface plasmon polariton (SPP) waves at the THz window [8]. In addition, graphene conductivity can be dynamically controlled with the use of an electric field applied via an external gate voltage which changes the chemical potential and hence the conductivity [9]. A big effort has been devoted to this research area for the past few years [10]. The main limitations of the graphene planar THz patch antenna are its low gain and bandwidth which can be significantly improved by several technologies such as meta surfaces and metamaterial structures MTM [11]. Metamaterials are engineering structures with properties not existing in nature. MTM are artificially constructed materials with an even negative value of permittivity, permeability, and refractive index for a band of frequency. Metamaterial structures can be capsulated in different applications such as biomedical applications [12], microwave filters [13], Terahertz absorber [14], Polarization splitters and refraction [15], and enhance antenna performance [16]. The gain of the planar microstrip patch antenna

[1] College of Engineering and Technology, Arab Academy for Science, Technology and Maritime Transport, Aswan 81511, Egypt, [2] Electrical Engineering Department, Faculty of Engineering, Aswan University, Aswan 81542, Egypt, Corresponding author: sherif.abdalla@aast.edu, e.hamad@aswu.edu.eg

https://doi.org/10.2478/jee-2022-0031, Print (till 2015) ISSN 1335-3632, On-line ISSN 1339-309X

Table 1. Graphene Properties, [7]

Property	Value
Transparency	$\sim$ 97.7%
Electronic mobility	$\sim 2\times10^5$ m^2/Vs
Current density	$\sim 10^9$ A/cm
Fermi velocity	$\sim 10^6$ m/s
Thermal conductivity	$\sim$ 5000 W/mK
Tensile strength	$\sim$ 1 TPa
Breaking strength	42 N/m
Elastic limit	$\sim$ 20%
Band gap	0
Surface area	2360 m^2/gm
Thickness	0.4–1.8 nm

could be much improved using MTM structures [17]. The metamaterials are also used to generate multi-band frequency windows [18]. One of the most important applications of metamaterial is the superstrate MTM on the patch antenna, it is used as a dielectric cover that protects the patch from environmental hazards. In addition to the protection purpose, superstrates have significant effects on the antenna performance like antenna gain, directivity, and radiation efficacy [19-22].

Herein, we are presenting a high-performance graphene patch antenna on Rogers 5880 ($\varepsilon_r = 2.2$) substrate at a 3.5 THz frequency band. The superstrate layer is used for enhancing the overall performance of the designed antenna as well as to protect the patch from environmental hazards. This patch is designed to resonate at a single frequency window, further; the metamaterial structure is utilized to make the antenna resonate at dual and Tri bands. The main contribution in this paper is the usage of dual-face superstrate MTM unit cell thats used to generate dual and tri resonant frequencies in the THz entire bandwidth with an acceptable antenna parameter such as gain, bandwidth, and radiation pattern with the latest published papers. Also, we discussed the performance of the antenna with the usage of different substrate material such as FR4, Rogers, polyamide, Arion and silicon dioxide in the THz frequency band thats has a vital effect on the material properties and also the main antenna performance.

2 Graphene material properties

Graphene is a single layer of graphite with a honeycomb hexagonal structure of carbon atoms. The extraction of one layer of graphene from the bulk graphite crystal structure was first carried out using a mechanical exfoliation technique. Over the decades, many other techniques have been used for graphene preparation synthesis. Such as chemical exfoliation, chemical vapor deposition (CVD), thermal exfoliation, and carbon segregation [7]. This extraordinary material has high mobility, high transparency, high flexibility, and high environmental stability at the THz frequency band. So, it is suitable material for usage in antenna applications. The graphene properties are indexed in Tab. 1.

3 Graphene conductivity

The SPP occurs when a high frequency of the electromagnetic wave is incident on a metal-dielectric interface. The graphene material is a good candidate that promotes the propagation of SPP waves, rather than the other nano-plasmonic materials such as gold and silver. Graphene is preferable due to its low loss and its high-quality factor.

The dispersion relation of transverse magnetic, TM of SPP depends heavily on graphene conductivity given by [9]

$$-i\frac{\sigma_s}{\omega\varepsilon_0} = \frac{\varepsilon_1 + \varepsilon_2 \coth(K_{\mathrm{SPP}} t_{\mathrm{ox}})}{K_{\mathrm{SPP}}}, \tag{1}$$

where ε_1 is the relative permittivity of the material over the graphene layer (air) and ε_2 is the second dielectric material below the graphene layer FR4, $t_o x$ is the material thickness, and K_{SPP} is the wavenumber of the SPP wave which can be expressed by

$$K_{\mathrm{SPP}} = K_0(\eta_{\mathrm{eff}}), \tag{2}$$

where η_{eff} is the effective refractive index of SPP and K_0 is the free space wavenumber $K_0 = 2\pi/\lambda$. The surface conductivity of graphene consists of two parts is calculated by Kubo's formula [23]

$$\sigma_s = \sigma_{\mathrm{ter}} + \sigma_{\mathrm{tra}}. \tag{3}$$

The intraband conductivity of graphene can be expressed as

$$\sigma_{\mathrm{tra}}(\omega) = -j\frac{2e^2}{\pi\hbar^2}\frac{\ln\left(e^{-\Lambda_c}+1\right)}{\omega - j\tau^{-1}}, \quad \text{with } \Lambda = \frac{\hbar\epsilon}{K_B T}, \quad \text{and } \Lambda_c = \frac{\mu_c}{K_B T}. \tag{4}$$

The interbond contribution is given by,

$$\sigma_{\mathrm{ter}}(\omega) = \frac{e^2}{4\hbar}\Big[H(\frac{\omega}{2}) + j\frac{4\omega}{\pi}\int_0^\infty \frac{H(\epsilon) - H(\frac{\omega}{2})}{\omega^2 - 4\epsilon^2}\mathrm{d}\epsilon\Big], \tag{5}$$

$$H(\epsilon) = \frac{\sinh\Lambda}{\cosh\Lambda_c + \cosh\Lambda}, \tag{6}$$

where T is the temperature, K_B is the Boltzmann constant, $\hbar$ is the reduced Planks constant, μ_c is the chemical potential, e is the charge of electron and τ is the relaxation time. According to Pauli exclusion principles, the interband conductivity can be neglected at a low THz range and the intraband of the graphene conductivity is the dominant part [24].

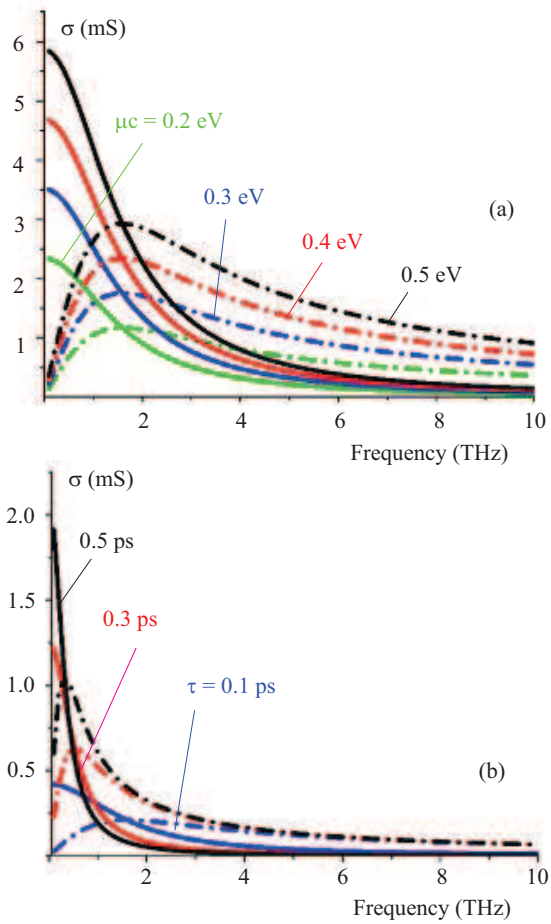

Fig. 1. Surface conductivity of graphene for: (a) – different chemical potential at $\tau = 0.1$ ps, T=300 K, and (b) – different relaxation time at $\mu_c = 0$ eV

4 Graphene modelling

Simulation and optimization of the graphene layer are performed using Finite Element Method (FEM)-based CST Microwave Studio. In this program, there are two built-in models of graphene, namely "graphene" and "graphene-Eps". In the first model, the graphene layer is a single layer with a thickness of 0.34 nm, the second one is a multilayer of graphene sheet with different values of thickness. In this work, we proposed an application of a single layer of graphene sheet of 0.34 nm thickness for our presented graphene plasmonic nanoantenna. Figure 1(a)(b) present the graphical representation for the surface conductivity of the graphene layer that is identical to the one presented in [25]. The real and imaginary parts of the simulated graphene for different values of chemical potential μ_c and relaxation time τ, respectively. These figures show that the total conductivity of a graphene slab is highly dependent on graphene chemical potential μ_c and relaxation time τ. The chemical potential depends on carrier density that can be controlled by an external gate voltage or chemical doping. Increasing the chemical potential μ_c leads to the increase of graphene surface conductivity. In addition, the antenna resonances shift to a higher frequency which enhances the flexibility of the tunable antenna design in the THz bands. The variation of μ_c enables the resonant frequency tunability features. The relationship between the chemical potential and gate voltage is explained by [26].

$$V_g = \frac{2e\mu_c^2}{\varepsilon\hbar\, v_f^2}, \tag{7}$$

where h is the substrate thickness and ε is the permittivity of the substrate material. The conductivity of graphene can be changed with the relaxation time (τ) as follows

$$\tau \simeq \mu_g \hbar \sqrt{\frac{n\pi}{e v_f}}, \tag{8}$$

where μ_g is the electron mobility of graphene and v_f is the Fermi velocity. The relaxation time increases with the chemical potential values. Long relaxation time supports the propagation of the SPP wave. For our graphene plasmonic nanoantenna designed in CST,we choose the following parameters: Temperature = 300 K, chemical potential $\mu_c = 0.4eV$,and relaxation time $\tau = 0.2ps$ .The graphene chemical potential (c) depends on the operating resonance frequency f_c of the antenna throughout the relation

$$\mu_c = E_f = \hbar\omega = hf_c. \tag{9}$$

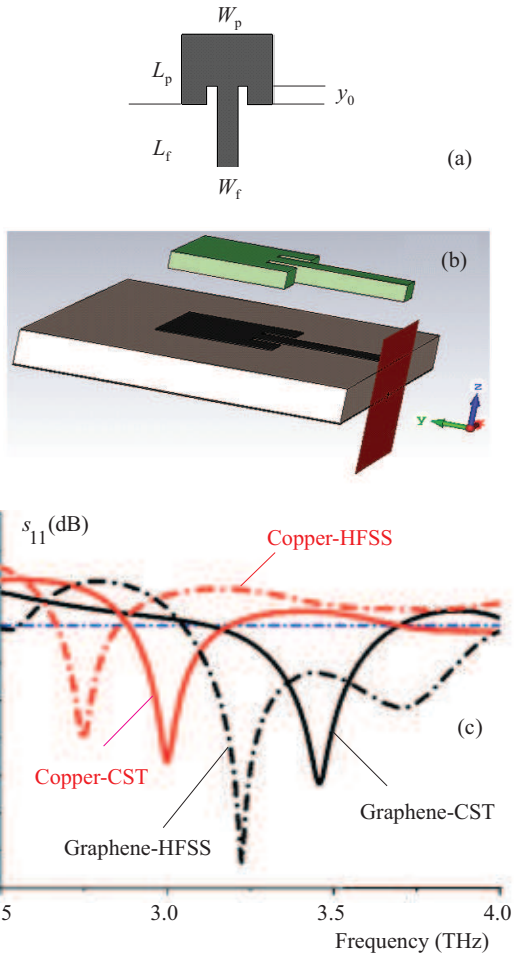

Fig. 2. The proposed patch antenna: (a) – schematic diagram, (b) – superstrate structure, and(c) – S_{11} of copper and graphene proposed antenna

Table 2. Dimensional parameters of the proposed antenna

Parameter	Value (m)
W_s	120
L_s	95
W_p	40
L_p	35
W_f	12
L_f	30
Y_0	8.3
h	10

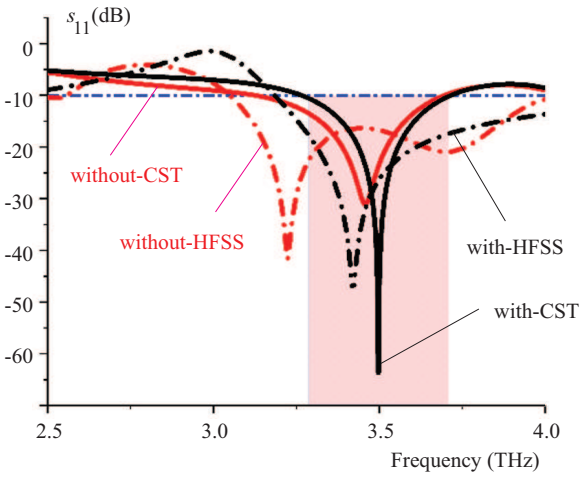

Fig. 3. S_{11} of curves of the antenna with and without superstrate layer

5 Antenna design and analysis

5.1 Conventional antenna

Graphene plasmonic microstrip patch antenna was designed by using a single layer of graphene radiating patch. The size is (40 μm$\times$35 μm) over a Rogers 5880 substrate material with a size of (120 μm $\times$95 μm), the thickness of $h_s = 10\mu$m and relative permittivity $\varepsilon_r = 2.2$. Table 2 shows the optimal dimensions of the graphene plasmonic antenna at 3.5 THz. The single element of the patch antenna is matched to a transmission line of 50 Ω characteristic impedance as shown in Fig. 2(a). The ground plane and the radiating patch of the antenna are designed using high conductivity of copper and graphene plasmonic material, respectively. Although copper has high electrical conductivity in RF and MW frequency bands, unfortunately, it changes in the THz frequency range. The skin depth and conductivity of copper decrease at lower bands of THz frequency consequently, the ohmic resistance part is the dominant contribution to the surface impedance of the copper, therefore antenna design has a significant challenge when it comes to the THz region. The decreases of the copper conductivity and skin depth in the terahertz frequency band lead to high losses in the propagation mechanism, hence degrading the radiation efficiency. The return loss of the antenna for copper and graphene materials is shown in Fig. 2(c). The optimized dimensions of the conventional patch antenna are tabulated in Tab. 2.

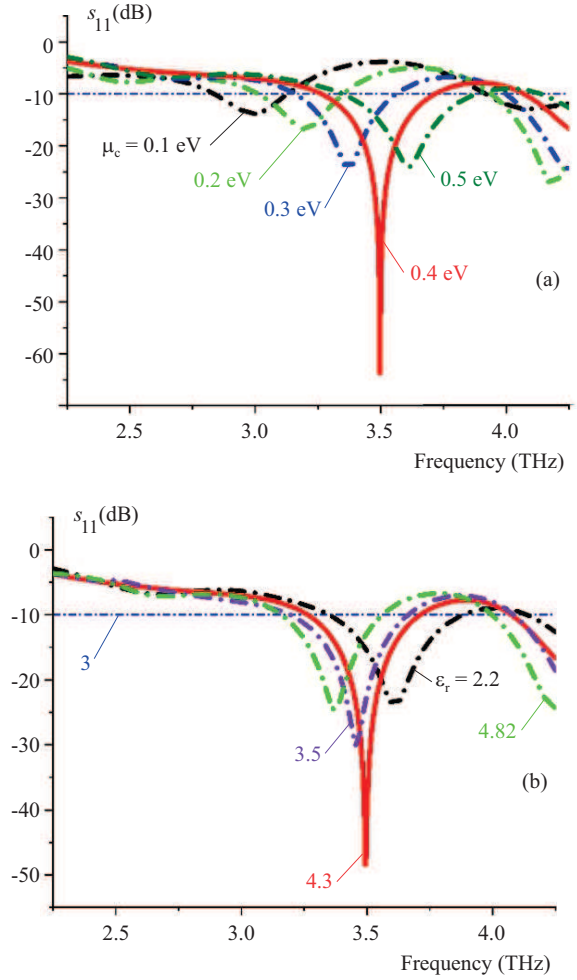

Fig. 4. S_{11} curves of the antenna for (a) – different chemical potential, (b) – different superstrate materials

5.2 Superstrate structure

As shown in Fig 2(b), the design of a rectangular patch antenna consists of a substrate layer over a ground plane of graphene material. The radiating patch is placed upon the substrate slab. A superstrate layer is placed upon the radiating patch with the same dimensions of the patch layer. Figure 3 shows the reflection coefficient S_{11} curves of the proposed graphene plasmonic antenna. The designed antenna operates at 3.5 THz without the superstrate layer having a Temperature of 300 K, chemical potential $\mu_c = 0.4\,$eV, and relaxation time $\tau = 0.4\,$ps, which gives a good S_{11} of – 35 dB and VSWR of 1.003. At the presence of a superstrate layer of FR4 ($\varepsilon_r = 4.3$) with a thickness of 10 μm placed upon the radiating patch, the overall effective dielectric constant of the radiating antenna has been slightly changed, consequently the resonant frequency is moved to 3.5 THz with an S_{11} of – 63.69 dB and VSWR 1.003 that makes the antenna perfectly matched.

The graphene chemical potential μ_c is dominantly decides the operating frequency of the designed antenna. This parameter varies from 0.1 eV to 0.5 eV and its effect

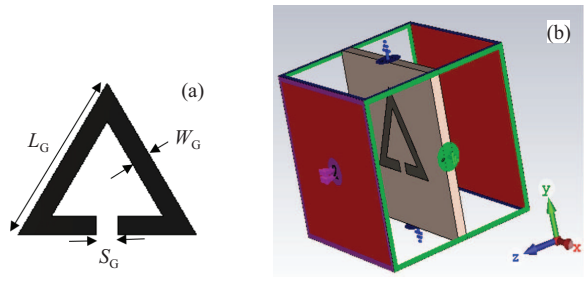

Fig. 5. G-TSRR unit cell(a) – schematic diagram, (b) – boundary conditions

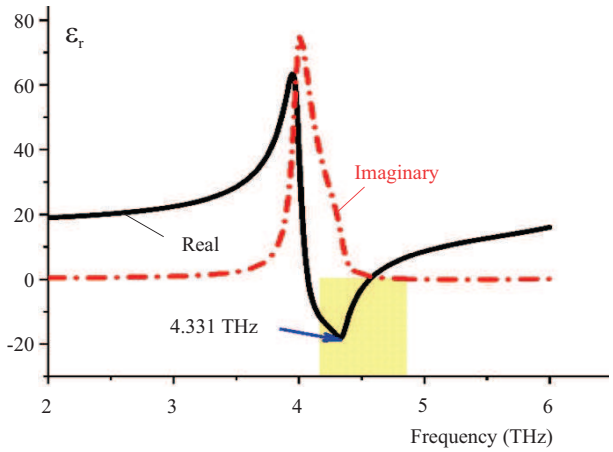

Fig. 6. The proposed G-TSRR unit cell – extracted relative permittivity

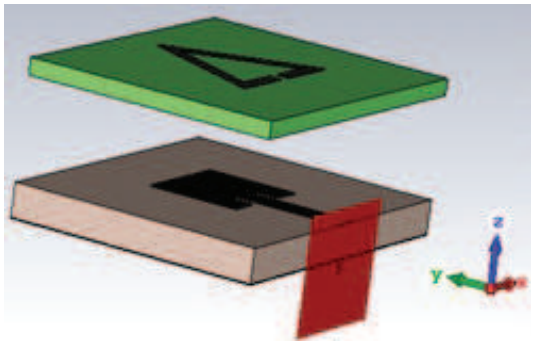

Fig. 7. Proposed antenna with superstrate MTM unit cell structure

on the S_{11} parameter is shown in Fig. 4(a). This graph informs us that, as the chemical potential increases, the frequency shifts to higher frequency; which agrees with that reported in [27]. At a value of 0.4 eV, S_{11} reaches its maximum value of -63.69 dB at 3.5 THz. Also, the chemical potential has a vital role in controlling the bandwidth of the antenna. As the chemical potential increases, the operating bandwidth will be increased as reported in [28]. In addition, we will check the proposed antenna validity for different dielectric materials for the superstrate layer. Fig. 4 (b), shows the reflection coefficient S_{11} curves for different superstrate materials. This figure illustrates that the dielectric constant of the material affects the value of the resonant frequency.

5.3 Graphene-based metamaterial design

The dual-band or multiband of the microstrip patch antenna is desirable, especially for THz frequency applications. So, different researchers were concerned with this point and used different methods to generate multi-frequency bands such as changing the substrate height or using different substrate materials of different permittivity beside each other. A more effective method used to generate multi-band frequency operation is the MTM structures. There are different shapes of the MTM, but the triangle split-ring resonator is an important unit cell that gives high-performance parameters such as return loss and bandwidth. Graphene-triangle split ring resonator (G-TSRR) unit cell was proposed to resonate at THz frequency having a structure and boundary conditions as illustrated in Fig. 5(a)(b), respectively. The geometrical dimensions of the unit cell are as follows: length of the triangle edge $L_G = 15\mu$m, width $W_G = 5\mu$m of the edge $S_G = 3\mu$m. According to $S-$ parameters the unit cell resonates at 4.33 THz with a reflection coefficient of – 45.6 dB. The negative permittivity characteristic of the G-TSRR unit cell has been extracted from the $S-$parameters as reported in [29]. It can be seen that the unit cell has a negative value at the desired operating frequency as depicted in Fig. 6.

5.4 Superstrate analysis with the MTM

As the Antenna performance is significantly influenced by the superstrate layer, a MTM superstrate unit cell (G-TSRR) is placed above the radiating patch as shown in Fig. 7. This layer is used to generate another resonance frequency in addition to the main resonance frequency of the antenna. The proposed unit cell is printed on an FR4 substrate material with a height of 3μm. The separated distance between the superstrate covering layer and the radiating patch is very important as it is controlling the antenna parameters. It can be investigated using the theory of Fabry-Perot Cavity [18]

$$d = \left(1 + \frac{\varphi}{\pi}\right)\frac{\lambda}{4}, \tag{10}$$

where φ is the reflection angle of the superstrate layer and d is the optimum spacing between the patch and the superstrate cover. In the previous works, the superstrate layer is designed to resonate at the same frequency of the main antenna to enhance the gain and bandwidth while, in this work, the superstrate layer is designed to resonate at different frequencies rather than the main frequency of the antenna to generate a dual-band structure. The $S-$parameter shown in Fig. 8(a), presents a dual resonance frequency at 3.503 THz is the main frequency of the antenna and at 4.331 THz is the resonance due to the graphene-metamaterial unit cell structure. The bandwidth of the two resonances is 400 GHz and 460 GHz, respectively. A parametric study is carried out to find the

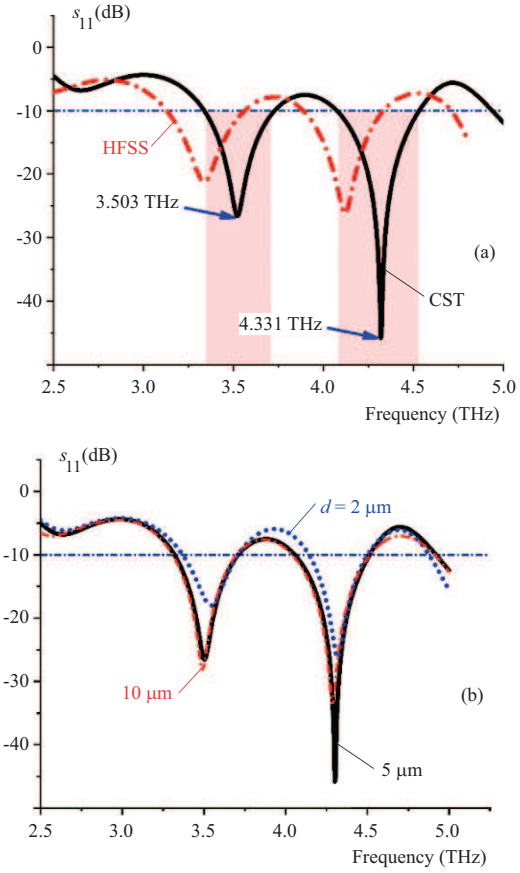

Fig. 8. S_{11} curves of dual-band MTM superstrate: (a) – verified by CST and HFSS, (b) – different superstrate distance height

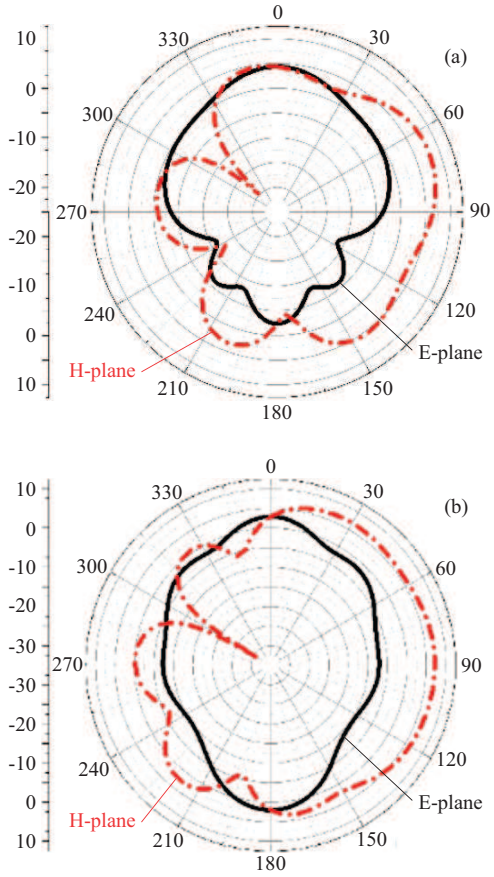

Fig. 9. E and H-planes of the dual-band MTM (a) – at 3.5 THz, (b) – at 4.331 THz

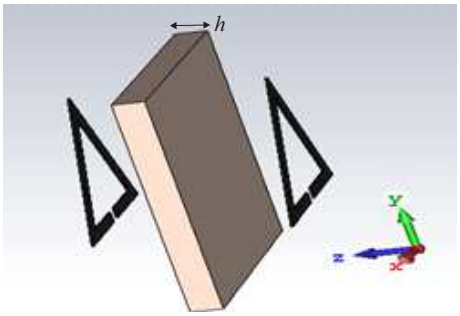

Fig. 10. Double-face MTM unit cell structure

optimum separated distance between the patch and the covering superstrate layer. This spacing is investigated through the S-parameter as illustrated in Fig.8(b). It can be seen that the optimum spacing d is about 5 μm above the patch. The E- and H-planes of radiation pattern at the two dual resonant frequencies at 3.5 THz and 4.331 THz are illustrated in Fig. 9(a,b). It can be seen that, the radiation pattern of E and H plane in the second resonant frequency in Fig. 9(b) has a wider beamwidth rather than in Fig. 9(a). These results are agreed with the S_{11} in Fig. 8 which gives a higher band width of 460 GHz.

5.5 Tri-band structure using double-face MTM unit cell

A design of a novel double-face graphene metamaterial unit cell using the same structure of the triangle split ring resonator is presented in Fig. 10. This structure is used as a superstrate layer over the patch antenna. It is used to generate a third resonance frequency at 2.32 THz besides, the other two frequencies at 3.53 THz and 4.38 THz. The structure of the Tri-band resonation is very interested in the new technologies of communication systems and aerospace applications. Massive iterations of the parametric studies were carried out to determine the optimum position and optimum dimensions of the designed MTM unit cell. The S-parameters of the Tri-band structure are presented in Fig. 11(a). It can be seen that the bandwidths of the dual-band frequencies are increased due to the double-face MTM superstrate structure. The bandwidths are 520 GHz and 610 GHz at 3.53 THz and 4.38 THz, respectively. In addition, a bandwidth of 230 GHz at the third resonance 2.32 THz has been achieved. This structure suffers from the frequency shift due to the coupling between the double-Face MTM unit cell. Although, it can be accepted as the shift is not divergent more about the main resonance of the proposed antenna at 3.5 THz and 4.331 THz. The substrate material of the superstrate layer is the same as the main antenna's substrate. One of the most effective parameters on the Tri-band reso-

Table 3. Graphene antennas with the other designs

Band	References	Frequency (THz)	S_{11} (dB) and resonance	VSWR	Gain (dB)	Bandwidth (GHz)
Single band	[30]	5.5	-65.32	1.001	3.91	217.7
	[31]	0.72	-59.97	1.007	-	270
	[32]	6.99	-75.66	1.0003	7.29	386
	[33]	2.6	-27	-	2.8	145.4
	[34]	0.99	-16.4	-	12.67	-
	Proposed work #1	3.5	-63.69	1.003	1.37	450
Dual band	[30]	4.33	-57.54	1.002	2.76	199.6
		5.82	-22.95	1.153	2.47	138.6
	[33]	2.48	-17	-	2.7	115.1
		3.35	-22	-	6.03	140.5
	[35]	1.96	-34	1.12	4.75	-
		4.83	-38	1.16	4.3	-
	Proposed work #2	3.50	-26.78	1.01	1.46	400
		4.33	-46.25	1.002	2.34	460
Tri-band	[35]	1.95	-26.32	1.12	4.79	-
		4.83	-24.84	1.14	5.05	-
		5.44	-19.61	1.23	5.53	-
	[36]	7.1	-30.49	1.05	4.91	2880
		11.1	-18.01	1.28	17.5	1580
		13.05	-22.01	1.17	11.6	1170
	Proposed work #3	2.32	-38.04	1.05	0.998	230
		3.53	-39.76	1.01	1.93	520
		4.38	-40.34	1.007	2.58	610

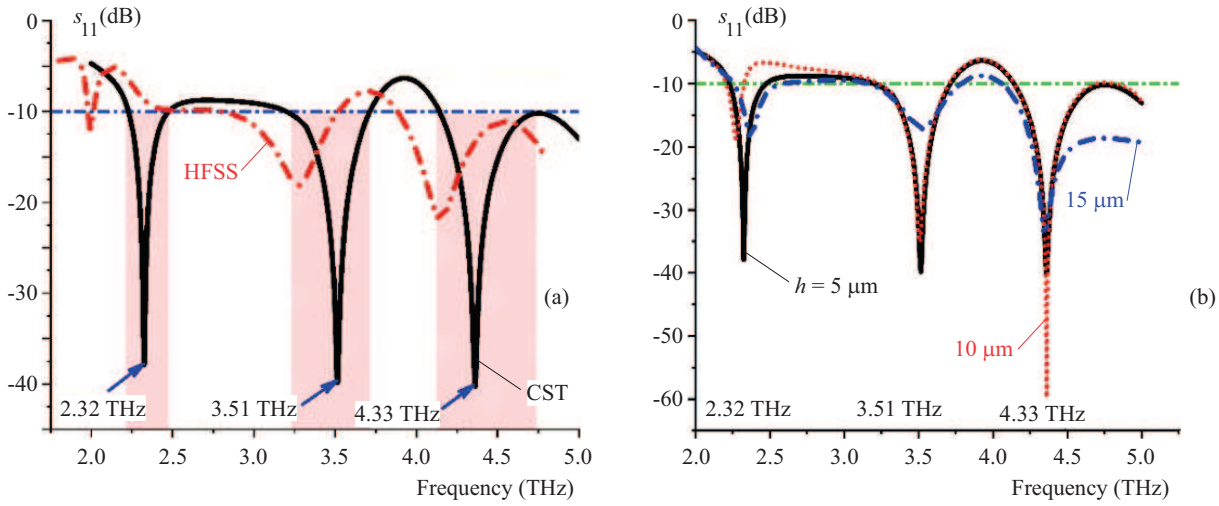

Fig. 11. S_{11} curves of Tri-band MTM superstrate: (a) – verified by CST and HFSS, (b) – different superstrate distance height

nance frequencies is the substrate height (h) thats can be affected by the coupling between the two elements of the MTM unit cells. The optimum height will be 5 μ m as shown in Fig. 11(b). It can be seen that the presence of the superstrate double-face MTM unit cell not only produces a different resonant frequency but also, enhances the gain and bandwidth of the designed antenna over the interested frequency band. The gain of the antenna without the usage of the MTM is about 1.37 dB at 3.5 THz. This value is enhanced by using the dual-band

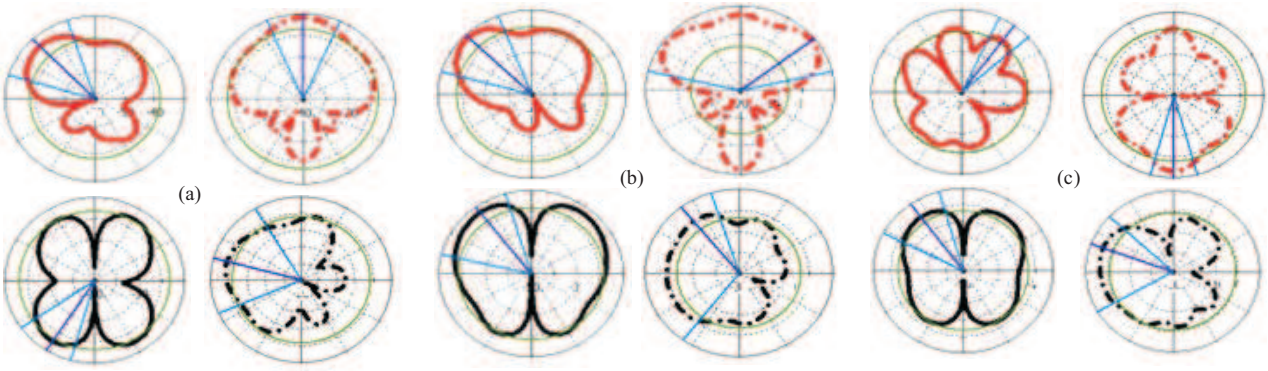

Fig. 12. Co and cross polarization of the tri-band structure: (a) – 2.32 THz, (b) – 3.53 THz, and (c) – 4.38 THz; E-plane red, H-plane black, Co-polarization -solid, Cross-polarization dashed

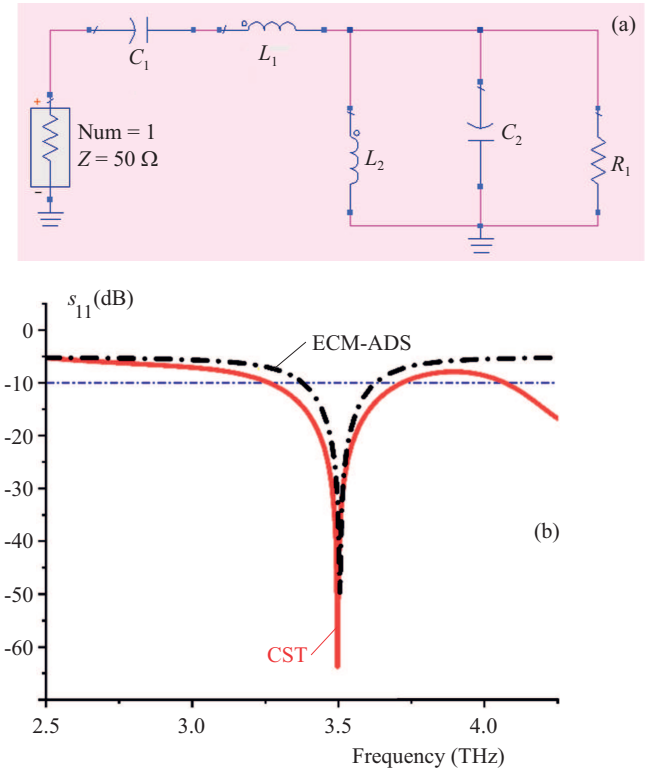

Fig. 13. (a) – ADS equivalent circuit model, (b) – S_{11} of ADS and CST graphene patch antenna

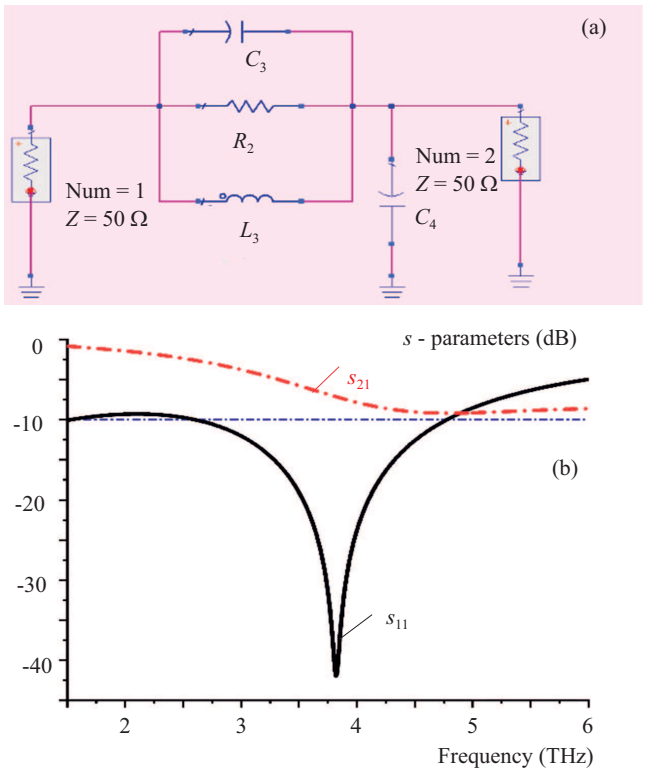

Fig. 14. (a) – ADS equivalent circuit model TSRR MTM, (b) – S_{11}, s_{21} of the unit cell

MTM unit cell as a superstrate layer so the gain will be 1.46 dB and 2.34 dB at 3.501 THz and 4.331 THz, respectively. The novel structure of the tri-band MTM unit cell over the patch is the optimum design that resonates at three different frequencies at 2.32THz, 3.53 THz, and 4.38 THz with a radiating gain of 0.998 dB, 1.93 dB, and 2.58 dB, respectively. A comparison between the overall antenna performances with the available latest literature is reported in Tab. 3. The MTM unit cell is used in different purposes such as increasing the gain, increasing the entire bandwidth, and generating other resonant frequencies. In our proposed structures, the graphene plasmonic double-face superstrate MTM unit cell is used to generate three resonant frequencies and also increases the bandwidth of the antenna. Furthermore, the gain of the proposed structures is kept constant with a little shift but not noticeable. Most of the reported structures have good results, while our proposed antenna using superstrate material is not only to enhance the antenna performance but, also, to produce another resonance frequency beside increase the antenna bandwidth.

As shown in Tab. 3, the proposed structure bandwidth is quite wide in the single, dual, and tri band designs, but in reference, the gain is high and the bandwidth is also high rather than the proposed structures this is due to the usage of different techniques of slots of bow tie antenna.

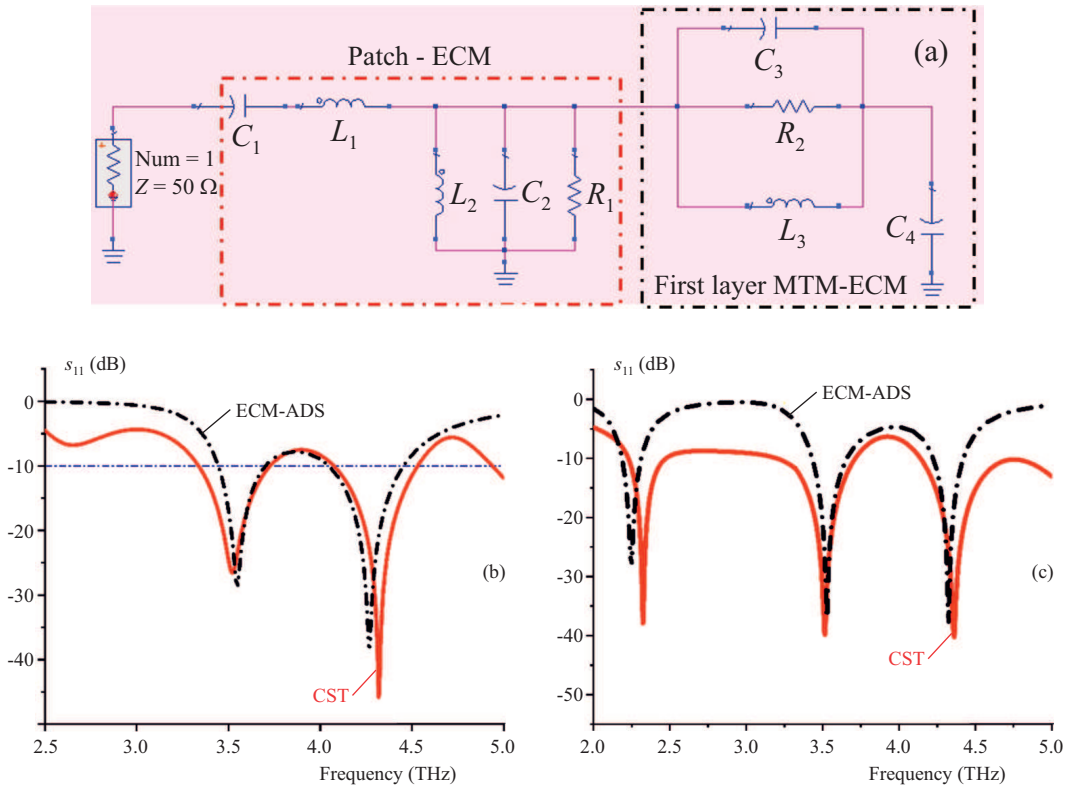

Fig. 15. (a) – ADS equivalent circuit model of single face MTM, (b) – S_{11} of CST and ADS of dual band, and (c) – S_{11} of CST and ADS of tri-band structure

Furthermore, introducing the double-face MTM structure generates is a new way to generate three-resonant frequencies in addition to increases the entire band width by keeping the gain in a satisfactory level. So that; this structure could be used for different applications in the THz frequency band. The tri-band structure has good gain, bandwidth, and radiation properties compared to the other references. The radiation pattern of the proposed antenna is shown in two planes, E-plane and H-plane as well as the Co-polarization and Cross- polarization at 2.32 THz, 3.53 THz, and 4.38 THz frequency are shown in Fig. 12. According to the radiation patterns, for the proposed antenna, we observe a stable radiation pattern the suggested antenna has semi bidirectional in H-plane and semi omnidirectional in the E- plane.

5.6 The equivalent circuit models

The equivalent circuit model (ECM) of the designed antenna structure is analyzed using ADS. The single patch antenna equivalent circuit model and the S11 parameters are illustrated in Figure 13(a, b). A comparison of the ADS software and the CST is introduced to make additional verification for the results. The ECM of the TSRR-MTM unit cell and its $S-$parameters are illustrated in Fig. 14(a, b). The Single face and double face MTM equivalent circuit model has been deduced using ADS software and the results give an asymptotic curve for single, dual and tri band structures as shown in Fig. 15 and Fig. 16. The optimal RLC values of the ECM are tabulated in Tab. 4.

Table 4. Lumped element component values of the equivalent circuit model

Parameter	Value (fF)	Parameter	Value (pH)
C_1	0.7	L1	2.6
C_2	3.1	L2	1
C_3	8.55	L3	0.2
C_4	8.55	L4	0.2
C_5	5.4	L5	3.5
C_6	0.62	$R_1 = R_2 = R_3$	145 Ω

6 Conclusion

In this article, a high-performance graphene microstrip patch antenna is investigated to operate at a frequency of 3.5 THz. A superstrate layer is proposed to cover the radiating graphene patch to protect the antenna from environmental threats and enhance the overall performance such as gain and bandwidth. A triangle split ring resonator unit cell MTM structure is printed above the superstrate layer over the patch to create another resonant frequency beside the main resonance of the antenna at

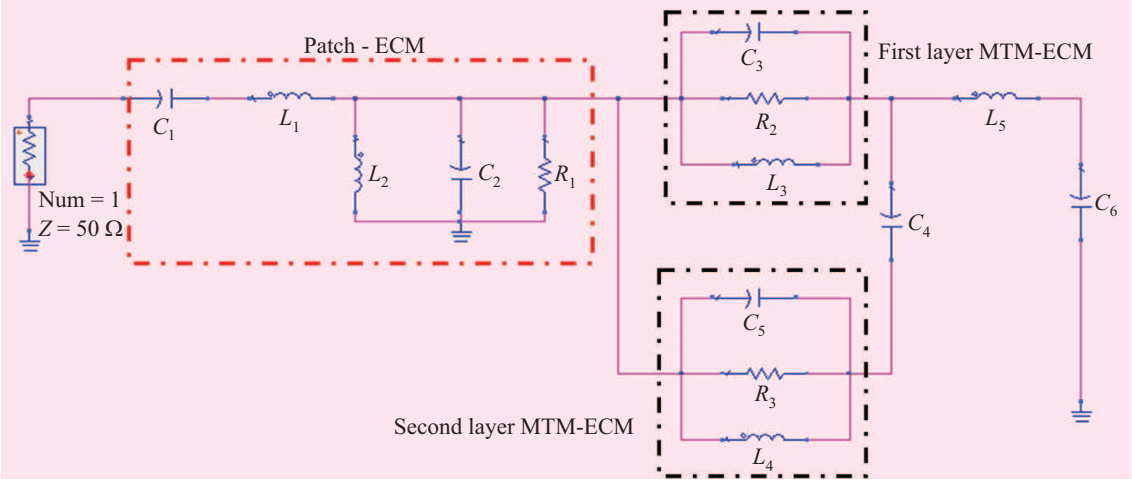

Fig. 16. ADS equivalent circuit model of graphene patch antenna with a double-face MTM unit cell

4.331 THz. The dual-band structure has a gain of 1.46 dB and 2.34 dB with a bandwidth of 400 GHz and 460 GHz at the resonant frequencies of 3.503 THz and 4.331 THz, respectively. A novel structure of double-face superstrate MTM is used to produce a third resonant frequency at 2.32 THz with a higher gain and bandwidth making it a good candidate for different applications in the THz frequency window. The proposed design of the antenna is re-simulated using HFSS to validate the results obtained from CST software. As observed from the S11 results, the agreement between the two software is moderated. This divergence between the two signals is due to the different calculation methods used in the CST and HFSS software.

References

[1] M. Alsabah, M. A. Naser, B. M. Mahmmod, S. H. Abdulhussain, M. R. Eissa, A. Al-Baidhani, N. K. Noordin, S. M. Sait, K. A. Al-Utaibi, and F. Hashim, "6G Wireless Communications Networks: A comprehensive survey", *IEEE Access*, vol. 9, pp. 148191 148243, 2021.

[2] L. Zhu, Z. Xiao, X.-G. Xia, and D. O. Wu, "Millimeter-Wave Communications With Non-Orthogonal Multiple Access for B5G/6G", *IEEE Access*, vol. 7, pp. 116123-116132, 2019.

[3] M. W. Akhtar, S. A. Hassan, R. Ghaffar, H. Jung, S. Garg, and M. S. Hossain, "The shift to 6G communications: vision and requirements", *Human-centric Computing and Information Sciences*, vol. 10, no. 1, 2020.

[4] Y. Luo, Q. Zeng, X. Yan, Y. Wu, Q. Lu, C. Zheng, N. Hu, W. Xie, and X. Zhang, "Graphene-Based Multi-Beam Reconfigurable THz Antennas", *IEEE Access*, vol. 7, pp. 30802-30808, 2019.

[5] S. A. Khaleel, E. K. I. Hamad, N. O. Parchin, and M. B. Saleh, "MTM-Inspired Graphene-Based THz MIMO Antenna Configurations Using Characteristic Mode Analysis for 6G/IoT Applications", *Electronics*, vol. 11, no. 14, pp. 2152, 2022.

[6] W. Ali, E. Hamad, M. Bassiuny, and M. J. R. Hamdallah, "Complementary split ring resonator based triple band microstrip antenna for WLAN/WiMAX applications", *Radioengineering*, vol. 26, no. 1, pp. 78-84, 2017.

[7] S. Dash, A. J. P. Patnaik, "Behavior of graphene based planar antenna at microwave and terahertz frequency", *Photonics and Nanostructures–Fundamentals and Applications*, vol. 40, pp. 100800, 2020.

[8] B. Zhang, J. M. Jornet, I. F. Akyildiz, and Z. P. Wu, "Mutual coupling reduction for ultra-dense multi-band plasmonic nano-antenna arrays using graphene-based frequency selective surface", *IEEE Access*, vol. 7, pp. 33214-33225, 2019.

[9] S. Dash, A. Patnaik, and B. K. Kaushik, "Performance enhancement of graphene plasmonic nanoantennas for THz communication", *IET Microwaves, Antennas & Propagation*, vol. 13, no. 1, pp. 71-75, 2019.

[10] A. A. A. Aziz, A. A. Ibrahim, and M. A. Abdalla, "Tunable Array Antenna with CRLH Feeding Network Based on Graphene", *IETE Journal of Research*, pp. 1-9, 2019.

[11] E. K. Hamad and A. J. R. Abdelaziz, "Performance of a metamaterial- based 1 2 microstrip patch antenna array for wireless communications examined by characteristic mode analysis", *Radioengineering*, vol. 28, no. 4, pp. 681, 2019.

[12] M. Puentes, M. Maasch, M. Schubler, and R. J. Jakoby, "Frequency multiplexed 2-dimensional sensor array based on split-ring resonators for organic tissue analysis", *IEEE Transactions on Microwave Theory and Techniques*, vol. 60, no. 6, pp. 1720-1727, 2012.

[13] A. H. Reja and S. N. Ahmad, "Design of Multiband Metamaterial Microwave BPFs for Microwave Wireless Applications", *Advances in Intelligent Informatics*, : Springer, pp. 179-192, 2015.

[14] D. Yan, M. Meng, J. Li, and X. Li, "Graphene-assisted narrow bandwidth dual-band tunable terahertz metamaterial absorber", *Front. Phys*, vol. 8, 2020.

[15] Y. Yuan, K. Zhang, X. Ding, B. Ratni, S. N. Burokur, and Q. Wu, "Complementary transmissive ultra-thin meta-deflectors for broadband polarization-independent refractions in the microwave region", *Photonics Research*, vol. 7, no. 1, pp. 80-88, 2019.

[16] W. Wu, B. Yuan, B. Guan, and T. Xiang, "A bandwidth enhancement for metamaterial microstrip antenna", *Microwave and Optical Technology Letters*, vol. 59, no. 12, pp. 3076- 3082, 2017.

[17] A. B. Abdel-Rahman and A. A. Ibrahim, "Metamaterial enhances microstrip antenna gain", *Microwaves and RF*, vol. 55, no, 7, pp. 46-50, 2016.

[18] E. K. Hamad, W. A. Ali, M. Z. Hamdalla, and M. A. Bassiuny, "High gain triple band microstrip antenna based on metamaterial super lens for wireless communication applications", *In-*

ternational Conference on Innovative Trends in Computer Engineering (ITCE), pp. 197- 204: IEEE, 2018.

[19] D. Li, Z. Szabó, X. Qing, E.-P. Li, and Z. N. Chen, "A high gain antenna with an optimized metamaterial inspired superstrate", *IEEE Transactions on Antennas and Propagation*, vol. 60, no. 12, pp. 6018-6023, 2012.

[20] P. Das, G. J. O. Varshney, "Analysis of tunable THz antennas integrated with polarization insensitive frequency selective surfaces", *Optical and Quantum Electronics*, vol. 53, no. 11, pp. 1-21, 2021.

[21] V. Dhasarathan, N. Bilakhiya, J. Parmar, M. Ladumor, and S. K. Patel, "Numerical investigation of graphene-based metamaterial microstrip radiating structure", *Materials Research Express*, vol. 7, no. 1, pp. 016203, 2020.

[22] P. Das and G. Varshney, "Gain enhancement of dual-band terahertz antenna using reflection-based frequency selective surfaces", *Optical and Quantum Electronics*, vol. 54, no. 3, pp. 1-23, 2022.

[23] G. W. Hanson, "Dyadic Green's functions for an anisotropic, non-local model of biased graphene", *IEEE Trans. Antennas and Propagation*, vol. 56, no. 3, pp. 747-757, 2008.

[24] X. Qin, J. Chen, C. Xie, N. Xu, and J. Shi, "A tunable THz dipole antenna based on graphene", *IEEE MTT-S International Microwave Workshop Series on Advanced Materials and Processes for RF and THz Applications (IMWS-AMP)*, pp. 1-3: IEEE, 2016.

[25] I. Llatser, *et al*, "Graphene-based nano-patch antenna for terahertz radiation, *Photonics Nanostruct.*, vol. 10, no. 4, pp. 353-358, 2012.

[26] M. Gatte, P. J. Soh, H. Rahim, R. Ahmad, and M. F. A. Malek, "The performance improvement of THz antenna via modeling and characterization of doped graphene", *Prog. electromagn. res. M*, vol. 49, pp. 21-31, 2016.

[27] M. J. Chashmi, P. Rezaei, and N. J. O. Kiani, "Reconfigurable graphene-based V-shaped dipole antenna: From quasi-isotropic to directional radiation pattern", *Optik*, vol. 184, pp. 421-427, 2019.

[28] H. B. Krid, Z. Houaneb, and H. Zairi, "Reconfigurable graphene annular ring antenna for medical and imaging applications", *Progress In Electromagnetics Research M*, vol. 89, pp. 53-62, 2020.

[29] R. W. Ziolkowski "Design, fabrication, and testing of double negative metamaterials", *IEEE Trans. Antennas and Propagation*, vol. 51, no. 7, pp. 1516-1529, 2003.

[30] M. A. K. Khan, T. A. Shaem, and M. A. Alim, "Analysis of graphene based miniaturized terahertz patch antennas for single band and dual band operation", *Optik*, vol. 194, pp. 163012, 2019.

[31] S. M. Shamim, M. S. Uddin, M. R. Hasan, and M. Samad, "Design and implementation of miniaturized wideband microstrip patch antenna for high-speed terahertz applications", *Journal of Computational Electronics*, vol. 20, no. 1, pp. 604-610, 2021.

[32] M. A. K. Khan, M. I. Ullah, R. Kabir, and M. A. Alim, "High- Performance Graphene Patch Antenna with Superstrate Cover for Terahertz Band Application", *Plasmonics*, vol. 15, pp. 1719-1727, 2020.

[33] M. Shalini and M. G. Madhan, "Design and analysis of a dual-polarized graphene based microstrip patch antenna for terahertz applications", *Optik*, vol. 194, pp. 163050, 2019.

[34] S. S. Efazat, R. Basiri, and S. V. Al-Din Makki, "The gain enhancement of a graphene loaded reconfigurable antenna with non–uniform metasurface in terahertz band", *Optik*, vol. 183, pp. 1179-1190, 2019.

[35] M. J. O. Shalini, "Performance predictions of slotted graphene patch antenna for multi-band operation in terahertz regime", *Optik*, vol. 204, pp. 164223, 2020.

[36] G. Bansal, A. Marwaha, A. Singh, R. Bala and S. Marwaha, "A triband slotted bow-tie wideband THz antenna design using graphene for wireless applications", *Optik*, vol. 185, pp. 1163-1171, 2019.

Received 16 June 2022

Sherif A. Khaleel received the BE and MSc degree in Electronic and Communication Engineering from Arab Academy for Science, Technology and Maritime Transport (AASTMT), Egypt in 2012 and 2017. He is currently working toward the PhD degree in the design a graphene microstrip patch antenna in the THz band for the 6G communication at the Faculty of Engineering, Aswan University, Aswan, Egypt. He is working now as a Teaching/Research Assistant at the college of Engineering and Technology, Department of Electronics and communication, AASTMT, Aswan- Egypt. His current research interests include the antenna design, metamaterials, and 6G communication, THz materials.

Ehab K. I. Hamad received the BSc and MSc degrees in electrical engineering from Assiut University, Egypt in 1994 and 1999, respectively and the PhD degree in electrical engineering from Magdeburg University, Germany in 2006. From 1996 to 2001 he was a Teaching/Research Assistant with the Aswan Faculty of Engineering, SVU, Egypt. From July 2001 to December 2006, he was a Research Assistant with the Chair of Microwave and Communication Engineering, University Magdeburg. From July 2010 to April 2011, he was with the School of Computing and Engineering, University of Huddersfield, UK as a Postdoctoral Research Assistant. He is currently a Full Professor for antenna engineering with Aswan University, Egypt. He has authored or coauthored over 60 technical peer-reviewed papers in international journals and conference proceedings. He is a supervisor on about 25 master and 13 PhD theses in different universities in Egypt. His current research interests include antennas, MIMO antennas, mm-wave antennas, 5G, MTM. He is also interested in designing microstrip antennas using the CMT as well as designing antennas in the THz frequency band using graphene plasmonic material.

Mohamed B. Saleh received his bachelor and master degrees in Electrical Engineering from Alexandria University, Egypt in 1966 and 1973, respectively. He received his PhD degree in Electronics Engineering from University Paul Sabatier de Toulouse/France, Jun 1979. He is a Principal Researcher and Supervisor of Solar Cells Research Projects. He is currently a full Professor for electronics in the department of electronics and communication engineering AASTMT-Aswan and President Counselor for International Affairs. Dr Mohamed participates in research projects at the national and international levels Solar Cells Fabrication Project Eindhoven University, HOLLAND Funded Project and Solar Cells Research Projects Ministry of industry and Academy of Scientific Research and Technology, Cairo EGYPT Funded Project. His current research interests include: solar cell fabrication and testing, Material Science Engineering, CNT and Graphene applications. He is working now on the THz application in microwave materials such as graphene and CNT also in the enhance the perovskite solar cell using different methods. He is a reviewer of many journals, international and national conferences.